Sensors & Actuators: A. Physical 370 (2024) 115232

Contents lists available at ScienceDirect

Sensors and Actuators: A. Physical

journal homepage: www.journals.elsevier.com/sensors-and-actuators-a-physical

Heavy metal sensing in plant and soil solutions using carbon fiber electrode

G M Hasan Ul Banna [a,b,*], James Siegenthaler [a,c], Antryg Benedict [d], Brendan Allen [c], Raul Murillo Martinez [e], Wei Zhang [d], Wen Li [a,b,c]

[a] Department of Electrical and Computer Engineering, Michigan State University, East Lansing, MI, USA
[b] Institute for Quantitative Health Science & Engineering, Michigan State University, East Lansing, MI, USA
[c] Fraunhofer USA Center Midwest, East Lansing, MI, USA
[d] Department of Plant, Soil and Microbial Sciences, Michigan State University, East Lansing, MI, USA
[e] Department of Mechanical Engineering, Michigan State University, East Lansing, MI, USA

ARTICLE INFO

Keywords:
Carbon Fiber Electrode
Heavy Metal Detection
Electrochemistry
Plant solution
Soil solution
DP-ASV

ABSTRACT

Analysis of trace level metals in environmental samples (e.g., soil, water, and plant samples) is important for assessing environmental quality and food safety. This paper reports a non-toxic, eco-friendly, and cost-effective sensing method, capable of in-situ detection of microgram per liter (μg/L) levels of heavy metal ions in plant and soil solutions using carbon fiber electrodes (CFEs) produced without using any microfabrication. The electrochemical behaviors of the CFEs were characterized by cyclic voltammetry (CV) and electrochemical impedance spectroscopy (EIS) measurements. As proof of principle, the CFEs were validated for sensing selected heavy metals in buffer solutions as well as in extracted plant and soil solutions using differential pulse anodic stripping voltammetry (DP-ASV). Experimental results confirm that the CFEs were able to simultaneously measure cadmium (Cd), lead (Pb), and mercury (Hg) with a detection limit of 2.10, 0.93, and 1.85 μg/L respectively in buffer solution, showcasing good selectivity and sensitivity. The ideal pH range for heavy metal detection was also extensively investigated and was found to be between pH 4.0 and pH 5.0. These findings lay a better foundation towards long-term and stable electrochemical analysis for plant and soil solution matrices.

1. Introduction

Heavy metal pollution in the environment is widespread worldwide, resulting from natural sources (volcanic eruptions, forest fires, rock weathering, etc.) and human activities (mining and smelting, industrial emission, fossil fuel combustion, etc.) [1,2]. Generally, metals with atomic densities higher than 5 g•cm^{-3} or five times or more greater than water density are considered heavy metals [3]. Some heavy metals are essential for life, and are not toxic in low quantities, such as iron (Fe), copper (Cu), zinc (Zn), and manganese (Mn). However, heavy metals such as cadmium (Cd), lead (Pb), and mercury (Hg) are considered toxic and biologically non-essential by the Environmental Protection Agency (EPA) [4]. Due to their toxicity, bioaccumulation, and environmental persistence, elevated levels of heavy metals in the environment pose major threats to ecosystem health and the safety of food crops grown with contaminated soil and water [5,6]. According to the World Health Organization (WHO), the human consumable limits of Cd, Pb, and inorganic Hg in bottled water are 5 μg/L, 1.5 μg/L, and 2 μg/L, respectively [7,8]. Consuming more than these limits can cause severe health issues including cancer, cardiac arrest, hypertension, renal disorder, kidney failure, and many other diseases [9–11]. A recent report from the 2021 US House of Representatives Subcommittee on Economic and Consumer Policy found high levels of Cd, Pb, and Hg in store-bought processed infant foods (vegetables and fruits), raising serious concerns about the potential neurocognitive impairment of infants and young children exposed to these toxic metals [12,13]. Therefore, there is a critical need for sensing techniques that can determine the trace levels of heavy metals in complex environments such as soil, water, and plants.

Conventional techniques for heavy metal detection including atomic absorption spectrometry (AAS), atomic fluorescence spectroscopy (AFS), inductively coupled plasma atomic emission spectrometry (ICP-AES), and mass spectrometry (ICP-MS) are generally accurate and some of these methods are highly sensitive with part per trillion (ppt) detection limits [14–18]. However, such methods are not practical for in-situ monitoring due to their sensitivity to mechanical vibration, calibration requirements, bulkiness, power consumption, and operating costs [18,

* Correspondence to: Michigan State University, Department of Electrical and Computer Engineering, 428 S Shaw Ln, Room 2120, East Lansing, MI 48823, United States.
E-mail address: bannag@msu.edu (G.M.H.U. Banna).

https://doi.org/10.1016/j.sna.2024.115232
Received 22 November 2023; Received in revised form 12 February 2024; Accepted 28 February 2024
Available online 1 March 2024

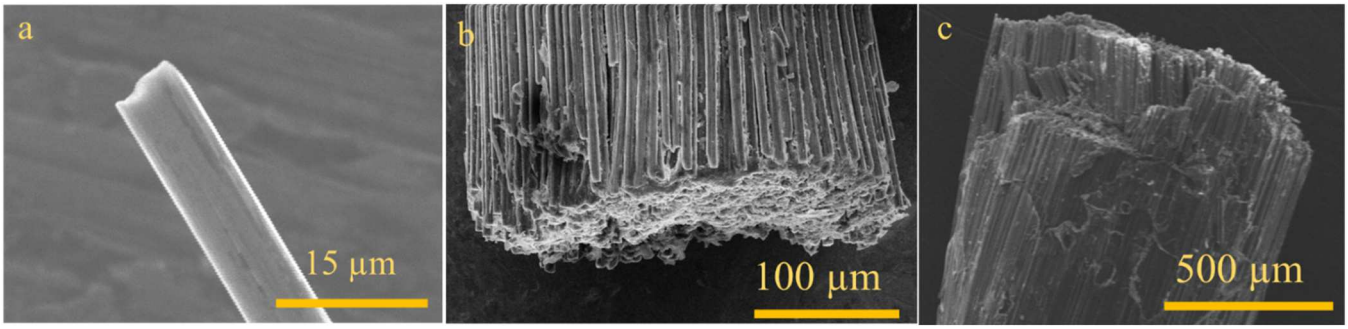

Fig. 1. SEM images of (a) 7.4 µm, (b) 0.28 mm, and (c) 0.94 mm carbon fibers.

19]. Additionally, they are laborious to use and require specifically trained personnel. Compared to conventional methods, electrochemical sensors have the advantages of reduced operational expenses, minimal power consumption, enhanced sensitivity, ease of operation, rapid analysis, portability, and applicability for field monitoring of environmental samples [20,21]. In particular, anodic stripping voltammetry (ASV) has demonstrated the capability to detect heavy metals at the sub-part per billion (ppb) level, making it a promising method for field analysis [15,22]. ASV involves two steps in the measurement sequence: a deposition step, where a negative potential is applied for a period of time, causing charged ions to become reduced at the electrode surface and form deposits. Then for the stripping step, a voltametric sweep from negative to positive potentials is applied so that deposited ions from the first step are oxidized and stripped off the electrode surface, resulting in a measured current response corresponding to each metal that was previously reduced. Liquid Hg is one of the most common electrode materials used for ASV heavy metal detection due to its ability to form homogenous, liquid metal amalgams. However, due to Hg's toxicity and environmental contamination concerns, solid metal electrodes such as bismuth (Bi), gold (Au), and platinum (Pt) have been studied by researchers as alternative electrode materials due to their low background currents, narrow stripping peaks, and low toxicity [23–26]. However, with metal electrodes, alloys may form between the analyte and electrode during the metal deposition process. As soon as metal ions are deposited, the surface properties of the electrode material change, and it is impossible to generate a defect-free pristine surface [24,27]. Alloy formation during the deposition step results in variable metal measurements, influencing both repeatability and long-term, in-situ metal monitoring systems [28–30]. Therefore, material that is chemically inert and non-metal is needed. Carbon-based materials are well known for being non-toxic, biocompatible, and resistance to alloy formation with metal, and lower background current [15,31]. Additionally, a carbon electrode's surface can be modified by synthetic chemistry methods, such as using a conductive polymer coating (i.e. Nafion), to improve sensitivity and selectivity of electrochemical analysis [32–35]. Various carbon materials including carbon nanomaterials such as carbon nanotubes (CNTs), graphene, graphene-oxides, and glassy carbons have been widely used to detect heavy metals [35–38]. However, these devices rely on sophisticated microfabrication facilities to form microfabricated electrodes, which renders the device fabrication both complex and costly. On the other hand, carbon fiber electrodes (CFEs) are less expensive, eco-friendly, and easy to fabricate without using a cleanroom fabrication facility. Moreover, the surface of CFEs can be made self-renewable by etching the outer surface [39]. This reduces surface fouling and enables prolonged sensing application by using a fresh electrode surface in each measurement. Over the past 30 years, CFEs have been popularly used for in-vivo neurochemical sensing applications by fast scan cyclic voltammetry (FSCV) [31,40,41]. A few researchers have explored using bismuth or antimony coated CFEs for heavy metal detection, but the applications of bare CFEs in environmental monitoring have been very limited [42,43].

In this study we demonstrated the use of bare CFEs as a non-toxic, eco-friendly, and cost-effective sensor for in-situ detection of microgram per liter (µg/L) levels of heavy metal ions in plant and soil solutions. The fabrication of CFEs is inexpensive and scalable and does not require sophisticated cleanroom microfabrication facilities. As a proof of principle, CFEs were tested for sensing selected heavy metals in buffer solutions as well as in 1:1 plant: buffer and soil: buffer solutions using differential pulse anodic stripping voltammetry (DP-ASV). Preliminary results confirm that the CFEs were able to simultaneously measure Cd^{2+}, Pb^{2+}, and Hg^{2+} with detection limits of 2.10, 0.93, and 1.85 µg/L, respectively, showcasing good selectivity and sensitivity. We also assessed the importance of the solution pH and found a pH range from 4.0 to 5.0 is needed for successful detection of heavy metals. Furthermore, CFE's prolonged measurement capability was tested and showed good repeatability in over 100 trials. This work will lay the foundation to develop new sensing technology for in-situ measurements of heavy metals in environmental media such as soil, plants, and water.

2. Materials

2.1. Experimental solutions and reagents

All reagents in this work were purchased from MilliporeSigma (Burlington, MA, USA), were analytical grade, and were used without purification unless otherwise noted. Heavy metal stock solutions were prepared by diluting Cd^{2+}, Pb^{2+}, and Hg^{2+} standard solutions of AAS grade (1000 ± 4 mg/l). Ferrocene carboxylic acid (FcCOOH) solution of 1 mM was prepared in 1 mM phosphate-buffered saline (PBS) (pH = 7.4). The pH of prepared solutions was determined and adjusted using a pH meter (Accumet, AB150, from Fisher Scientific, USA). The total carbon (TC) in soil and plant solutions were measured using a total organic carbon (TOC) instrument (Liquid TOC II, Elementa, Hanau, Germany). Additionally, all the aqueous solutions were prepared with deionized (DI) water with a resistivity of 18.2 MΩ cm at around 21 °C and TOC of < 5 ppb (Barnstead™ GenPure™ xCAD Plus Ultrapure Water Purification System, Thermo Scientific).

2.2. Carbon fibers

Single AS4 carbon fiber strands with a diameter of 7.4 µm were purchased from Hexcel Corporation (Hexcel, Stamford, CT) and have a resistivity of 1.7×10^{-3} ohm-cm and 94% carbon content. Carbon fiber composite rods with 0.28 mm and 0.94 mm diameters were purchased from CST-The Composites Store, Inc (Tehachapi, CA, USA). These composite rods were constructed by binding together multiple strands of T700S carbon fibers (resistivity 1.6×10^{-3} ohm-cm) with a bisphenol epoxy, producing rods with a fiber volume of 63% and 60% for the 0.28 mm and 0.94 mm rods respectively. Optical microscope (NIKON Eclipse LV100ND, Nikon Corp., Tokyo, Japan) and scanning electron microscopy (SEM) (Hitachi S-4700, Hitachi Ltd., Tokyo, Japan) were used to characterize the surface morphology of the carbon fibers. Fig. 1

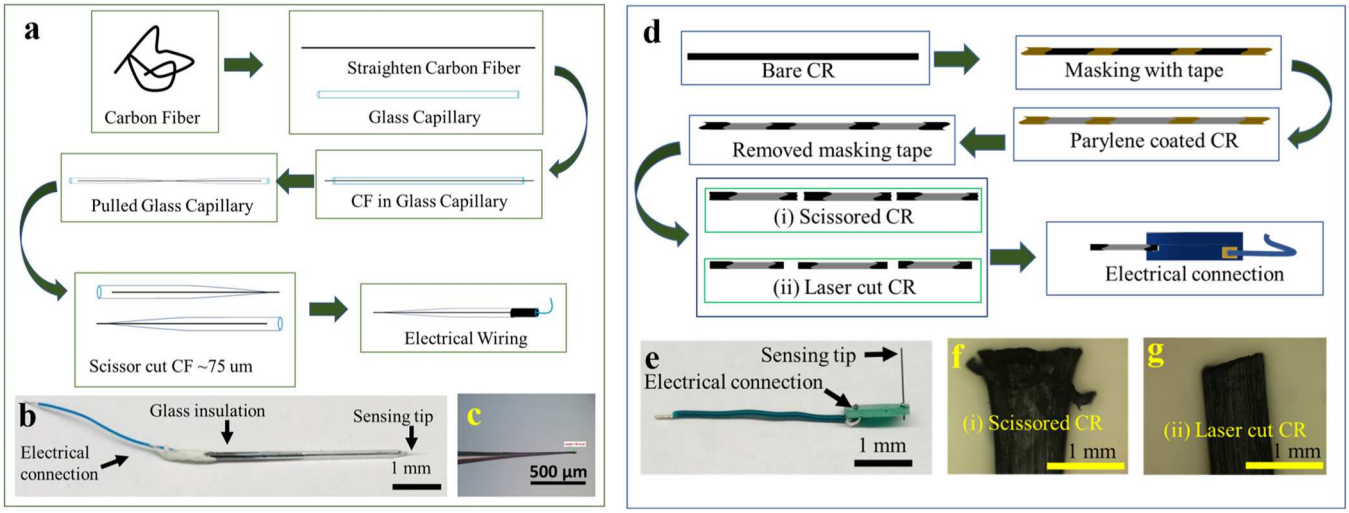

Fig. 2. Fabrication process of (a) 7.4 µm (d) 0.28 mm and 0.94 mm diameter CFE.

shows the SEM image comparison of three different carbon fibers with diameters (a) 7.4 µm, (b) 0.28 mm, and (c) 0.94 mm. Fig. 1(b) and (c) confirms that the thicker fibers are composed of a bunch of thinner carbon fibers, bound together.

2.3. Soil and plant solutions

Soil solutions for heavy metal sensing were prepared from a soil sample collected from the Michigan State University Research and Teaching Farm located in East Lansing, Michigan, USA. The soil is a sandy clay loam (pH 8.8, organic carbon 2.8%, clay 23.9%, silt 21.4%, and sand 54.7%) [44]. The plant solution was prepared using romaine lettuce leaves purchased from Whole Foods (Whole Foods Market Inc., TX, USA). The soil sample was collected from the top 15 cm depth, air-dried, ground, and then passed through a 2-mm sieve before it was used to prepare the soil solution. To prepare the plant solution, the fresh lettuce leaves were first washed with DI water to remove any soil or unwanted particulates. The leaves were then weighed and diced into small pieces. To create both the soil and plant solutions, 100 g of the soil sample or the diced lettuce leaf sample were suspended into 1 L of DI water and mixed for 24 hours. The solutions were then passed through Whatman grade 2 filter paper. The supernatant was collected and filtered using a 0.22 µm polytetrafluoroethylene (PTFE) membrane and vacuum filtration. Finally, the collected solutions were then utilized in the subsequent experiments. The soil solution was grayish, and the plant solution was greenish after processing. Graphical illustration of the preparation process is included in Figure S3.

3. Experimental methods

3.1. Carbon fiber electrode fabrication

Carbon fiber electrodes (CFEs) were fabricated in an open lab environment following two methods without using any microfabrication. The purchased CFEs were cleaned using acetone, methanol, and DI water bath for 5 minutes and then used without any modifications. In the first method, the 7.4-µm diameter single carbon fiber was used to fabricate CFEs following the procedure described elsewhere [45]. Briefly, the carbon fiber was inserted into a glass capillary (World Precision Instruments Sarasota, FL, USA) using a vacuum pump. After aspiration, the capillary was pulled on a commercial puller (Stoelting Co, Wooddale, IL), resulting in a tapered seal around the single carbon fiber. The sensing area of the electrode was controlled by the extruded carbon fiber length and cut to ~100 µm from the edge of glass seal. The other side of the fiber was electrically connected to a wire using a conductive graphite adhesive for electrical connection with the electrochemical station, as shown in Fig. 2(a). Fig. 2(b) shows the photograph of the fabricated CFE. Fig. 2(c) shows the microscopic image of sensing tip of the fabricated 7.4 µm diameter CFE.

For the second method, the 0.28 mm and 0.94 mm diameter carbon fibers were used. The CFEs were fabricated by wrapping the carbon fibers with a masking tape so that some parts of the carbon fibers were exposed, and some parts were covered with the tape. Then a 2 µm layer of parylene-C (a non-conductive coating) was conformally deposited over the carbon fibers in open lab environment using a PDS 2010 Labcoter® 2 (Specialty Coating Systems). Later, the masking tape was removed mechanically, and the CFs were hand-cleaved or laser cut so that both sides were exposed and the middle was covered with parylene-C. Scissors were used to hand-cleave the CFs and a femtosecond (FS) laser (Astrella-USP-1 K, Coherent Corp. Santa Clara, CA, USA) with wavelength $\lambda = 800$ nm, frequency $f = 1$ kHz, and power $P = 5$ W was used to laser cut the CFs. Finally, one exposed side was connected to a printed circuit board (PCB) using the conductive carbon adhesive while the other was used as a sensing electrode as shown in Fig. 2(d). For these CFEs, the cross-sectional areas of the cleaved fibers are the electrode sensing area. Fig. 2(e) shows the photograph of the fabricated CFE. Fig. 2 (f) and (g) show the microscopic image of the 0.94 mm diameter CFE sensing tip and the difference between hand cleaved and laser cut CFs. It is noted that the laser cut CF provides a smoother cutting edge compared to the hand cleaved.

3.2. Electrochemical measurements

All the electrochemical measurements were taken using CH Instruments (CHI6149E) potentiostat (CH Instruments, Inc. Austin, USA) in a three-electrode mode. The CFE was used as a working electrode (WE), an Ag/AgCl electrode (purchased from CH Instruments, Inc. Austin, USA) as a reference electrode (RE), and a Pt wire as a counter electrode (CE). In particular, DP-ASV was performed to validate the heavy metal sensing performance of the CFEs as follows: a plating deposition of −0.7 V for 120 s, followed by a voltage stripping ramp up to 0.8 V with a frequency of 60 Hz, an amplitude of 40 mV, and an increment voltage of 2 mV. These values are effectively chosen so that the targeted heavy metals can successfully detect, and carbon fibers are not over oxidized [40]. To estimate the effective sensing area of the CFEs, cyclic voltammetry (CV) was done in a 0.5 mM $K_3[Fe(CN)_6]$ solution containing 0.1 M KCl with 0.1 M acetate buffer solution (pH = 5.0) with varying scan rates. Electrochemical behavior and electrical

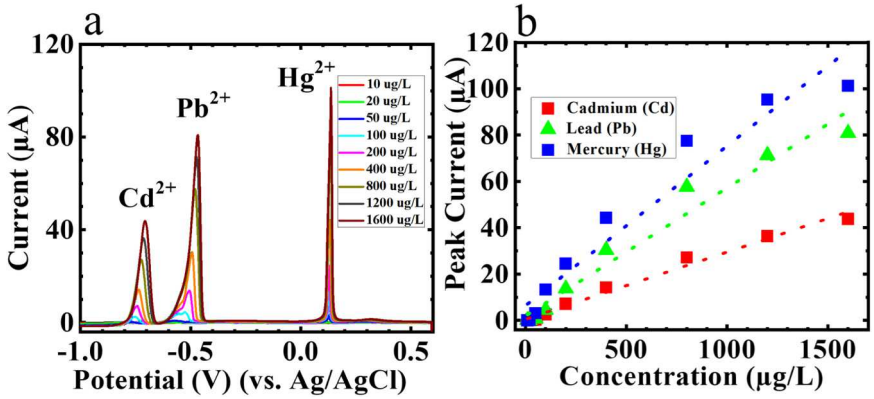

Fig. 3. (a) Detection of 10, 20, 50, 100, 200, 400, 800, 1200, and 1600 μg/L concentration of Cd^{2+}, Pb^{2+}, and Hg^{2+} mixture in 0.01 M acetate buffer (pH=4.97) solution containing 50 mM NaCl with CFE as WE. (b) Linear calibration curve in the mixture solution of Cd^{2+}, Pb^{2+}, and Hg^{2+} from 10 to 1600 μg/L (n=1).

conductivity of the CFEs were investigated by electrochemical impedance spectroscopy (EIS) using typical Nyquist plot analysis [46]. The measurements were taken at 5 mV perturbation amplitude in the frequency range of 1–10^5 Hz in a 0.01 M acetate buffer (pH=4.97) solution containing 50 mM NaCl. All electrochemical experiments were run at room temperature inside a custom-made Faraday cage to minimize external electrical noises and all potentials reported are against the Ag/AgCl RE.

3.3. Statistical analysis

All data plots and means and standard deviations were performed using OriginLab (OriginLab Corporation, MA, USA). Limit of detection (LOD), limit of quantification (LOQ), and spider charts were constructed using Microsoft Excel (Microsoft Corporation, WA, USA).

4. Results and discussion

4.1. Sensing performance of hand cleaved CFEs

The 0.94 mm hand cleaved CFE was used to detect Cd^{2+}, Pb^{2+}, or Hg^{2+}individually in the 50 ml solutions of 0.01 M acetate buffer (pH = 4.97) containing 50 mM NaCl and 100–1200 μg/L of the individual metal to determine the corresponding potential with respect to Ag/AgCl RE. Distinguishable peaks at −0.75 V, −0.5 V, and +0.12 V were observed for Cd^{2+}, Pb^{2+}, and Hg^{2+} respectively in DP-ASV voltage vs current plots. It is important to note that adding heavy metals changed the solution pH value from 4.97 to 4.61 as the concentration increased due to the acid in the metal standards. A detailed assessment of pH changes with varying concentration and solution type was completed (Table S1). It was found that the variation of pH values in buffer solution did not influence the respective peak potentials for Cd^{2+}, Pb^{2+}, and Hg^{2+}. However, the pH can highly influence heavy metal detection, which has been extensively analyzed in the later part of this paper.

After determining the individual metal potentials, DP-ASV was repeated on mixtures of the metals in the 0.01 M acetate buffer (pH = 4.97) containing 50 mM NaCl solution with 10–1600 μg/L of each metal. Fig. 3(a) shows that three peaks at around −0.75 V, −0.5 V, and +0.12 V were detected for Cd^{2+}, Pb^{2+}, and Hg^{2+}, respectively, in one single DP-ASV measurement. This represents good selectivity over the range of heavy metal concentrations. The amplitude of the current peak is linearly related to the concentration with R^2 of 0.986, 0.964, and 0.941 for Cd^{2+}, Pb^{2+}, and Hg^{2+} respectively (n=1), as demonstrated in Fig. 3(b).

For the analytical process, the limit of detection (LOD) and the limit of quantification (LOQ) are two important parameters to assess the sensitivity of analytical performance of the sensors. These two parameters can be calculated using the calibration curve obtained from the DP-ASV's linear range response based on the following equations:

$$\mathrm{LOD} = 3\frac{SD}{b} \text{ and } \mathrm{LOQ} = 10\frac{SD}{b}$$

where S_D is the standard deviation of blank solutions and b is the slope of the calibration plot [47]. The calculated LOD and LOQ for the three metals are summarized in Table 1.

Table 1
Sensitivity, LOD, and LOQ of 0.94 mm CFE in 0.01 M acetate buffer (pH=4.97) solution containing 50 mM NaCl (n=3).

Metals	Slope/ Sensitivity (μA/(μg/L))	R^2 value	LOD (μg/L)	LOQ (μg/L)
Cd^{2+}	0.0289 ± 0.001	0.986	2.10	7.01
Pb^{2+}	0.055 ± 0.004	0.964	0.93	3.09
Hg^{2+}	0.069 ± 0.007	0.941	1.85	6.17

4.2. Effect of electrode area on sensing performance

Electrochemical measurements were performed using cyclic voltammetry (CV) in 0.5 mM $K_3[Fe(CN)_6]$ containing 0.1 M KCl with 0.1 M acetate buffer solution (pH = 5.0). Voltammograms were collected at increasing scan rates of 0.01 V/s, 0.02 V/s, 0.05 V/s, 0.1 V/s, 0.2 V/s, and 0.5 V/s for a hand cleaved 0.94 mm diameter CFE (Fig. 4(a)). By plotting both the oxidation and reduction response of this CFE, it was found that the current maintained a linear relationship with scan rate (Fig. 4(b)) indicating an adsorption-controlled process. We further compared the response of $Fe(CN)_6^{-3}$ on the three different electrode materials, the 7.4 μm, 0.28 mm, and 0.94 mm Ø CFEs, measured at a scan rate of 0.01 V/s (Fig. 4(c)). A large capacitive response was observed for the 0.94 mm Ø CFE, which is attributed to the higher electrochemical surface area compared to the other two fibers, and the increased capacitance due to the bisphenol epoxy adhering the individual fibers together for the thicker fiber. The other two CFEs showed a far smaller response in current magnitude. Impedance characterization (Fig. 4(d)) of the three electrodes showed a comparable response for the 0.28 mm and 0.94 mm diameter CFEs. However, the impedance output of the 7.4 μm Ø CFE was significantly higher, mainly because it has the smallest electroactive area and lacks the binding agent that is used in the larger CFE rods.

The effective areas of 7.4 μm, 0.28 mm and 0.94 mm Ø CFEs were calculated electrochemically by measuring the response of 0.5 mM $K_3[Fe(CN)_6]$ at varying scan rates of 0.01 V/s, 0.02 V/s, 0.05 V/s, 0.1 V/s, 0.2 V/s, and 0.5 V/s using the Randles-Sevcik equation [48,49].

$$i_p = 2.69x10^5 n^{\frac{3}{2}} A D^{\frac{1}{2}} C v^{\frac{1}{2}}$$

where i_p is the cathodic peak current, n is the number of transported

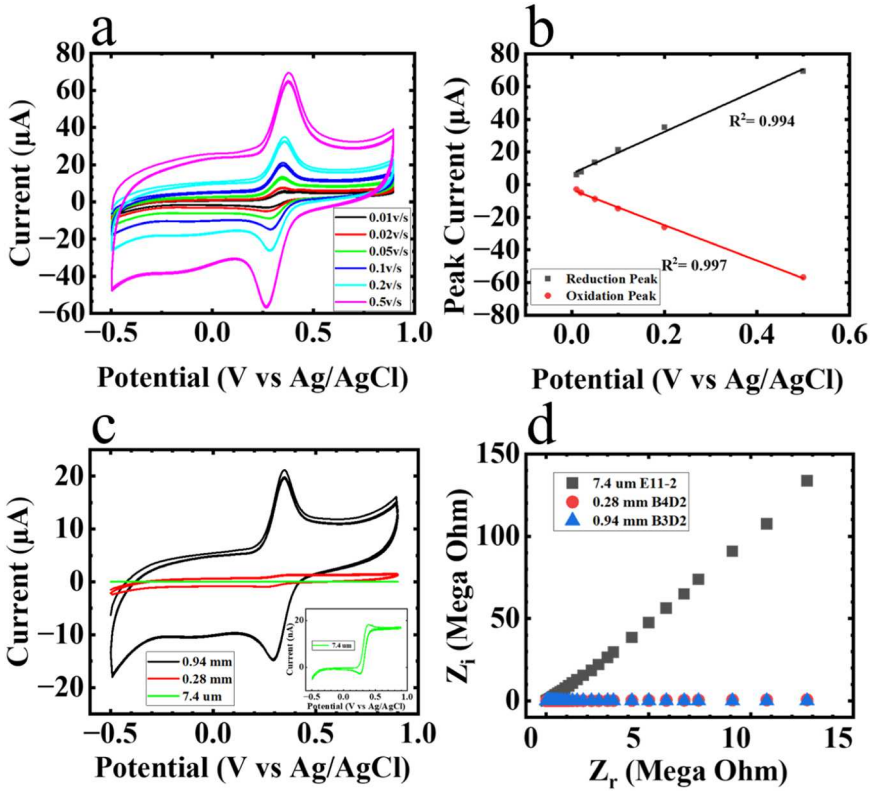

Fig. 4. Cyclic voltammograms of (a) 0.94 mm diameter CFE with scan rate of 0.01 V/s, 0.02 V/s, 0.05 V/s, 0.1 V/s, 0.2 V/s, and 0.5 V/s. (b) Peak oxidation and reduction current in varying scan rates (c) CV comparison between 7.4 μm, 0.28 mm, and 0.94 mm Ø CFE in 0.5 mM $K_3[Fe(CN)_6]$ containing 0.1 M KCl with 0.1 M acetate buffer solution (pH=5.0) at scan rate 0.01 V/s (d) EIS spectrum comparison of 7.4 μm, 0.28 mm and 0.94 mm Ø CFE in 0.01 M acetate buffer (pH=4.97) solution containing 50 mM NaCl.

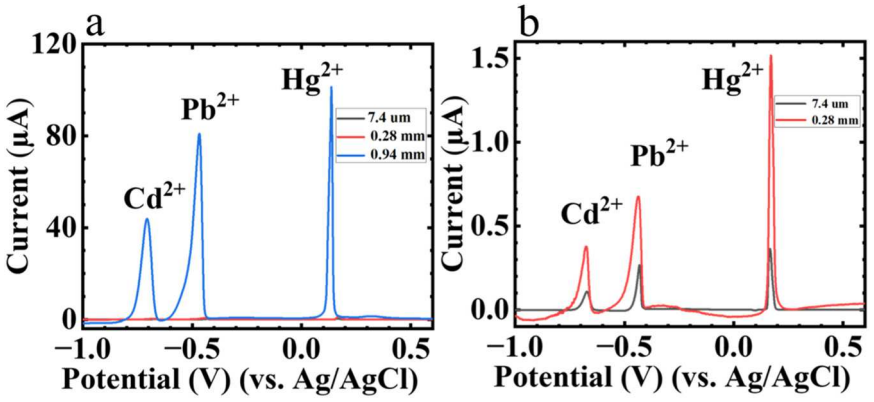

Fig. 5. (a) Peak current of 7.4 μm, 0.28 mm and 0.94 mm Ø CFE's at 1600 μg/L Cd^{2+}, Pb^{2+}, and Hg^{2+} respectively in in 0.01 M acetate buffer (pH=4.97) containing 50 mM NaCl. (b) Enlarged graph for the peak current response of heavy metals sensing with 7.4 μm and 0.28 mm Ø CFE.

electrons, A (cm^2) is the effective electrochemical surface, D ($cm^2 \cdot s^{-1}$) is the diffusion coefficient, C ($mol \cdot cm^{-3}$) is the concentration of redox species, and ν ($V\ s^{-1}$) is the potential scan rate. The dependency of the anodic peak potentials on the natural logarithm of the potential scan rate was investigated and linear fit lines were generated using the cathodic peak current and the square root of the potential scan rate. Using this method, the effective areas of the 7.4 μm, a 0.28 mm and 0.94 mm diameter CFEs were estimated to be around 2.27×10^{-5} cm^2, 8.57×10^{-3} cm^2, and 1.23×10^{-1} cm^2, respectively.

To study the effect of electrochemical effective area of CFEs on sensing performance, DP-ASV was performed in the buffer solution with a 1600 μg/L concentration of Cd^{2+}, Pb^{2+}, and Hg^{2+}. As shown in Fig. 5 (a), with the increasing effective area, the peak heights for each metal increased dramatically, indicating better sensitivity of the CFE. For example, for Cd^{2+} the sensing peak current of the 0.28 mm CFE is 3.5x and the 0.94 mm CFE is 400x higher than their 7.4 μm counterpart. Table S2 summarizes the peak currents of Cd^{2+}, Pb^{2+}, and Hg^{2+} using different diameter CFEs.

Electrochemical behaviors of all the three types of CFEs are comparable. Furthermore, due to the higher surface area, the 0.94 mm Ø CFE yielded higher detection current responses compared to other Ø CFEs. Therefore, from now on in this paper we choose to report the 0.94 mm Ø CFE's performances for simplicity.

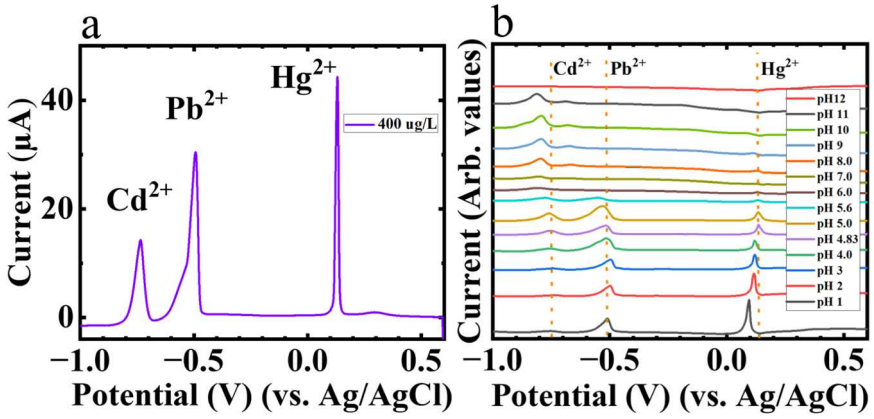

Fig. 6. (a) Detection of 400 μg/L concentration of Cd^{2+}, Pb^{2+}, and Hg^{2+} in 0.01 M acetate buffer (pH=4.83) solution containing 50 mM NaCl with CFE as WE. (b) Detection of Cd^{2+}, Pb^{2+}, and Hg^{2+} at 400 μg/L concentration solution, with varying pH from 1.0 to 12.0.

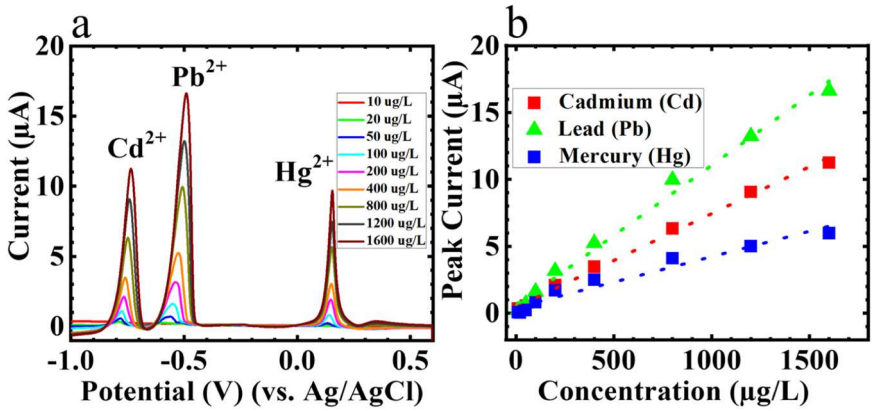

Fig. 7. (a) Detection of 10, 20, 50, 100, 200, 400, 800, 1200, and 1600 μg/L concentrations of Cd^{2+}, Pb^{2+}, and Hg^{2+} mixture in soil solution (pH=5.03) with CFE as WE. (b) Linear calibration curves in the mixture solution of Cd^{2+}, Pb^{2+}, and Hg^{2+} from 10 to 1600 μg/L (n=1).

4.3. Effect of pH on sensing performance

The effect of the buffer solution pH on heavy metal detection performance was investigated extensively in this work. At first, 400 μg/L of Cd^{2+}, Pb^{2+}, and Hg^{2+} were added to the acetate buffer solution (pH=4.83) and were measured using DP-ASV with the 0.94 mm hand cleaved CFE. Fig. 6(a) shows three distinct peaks for Cd^{2+}, Pb^{2+}, and Hg^{2+} at −0.75 V, −0.5 V, and +0.12 V, respectively. Then to change the pH value of the solution, either 1 M of hydrochloric acid or 1 M of sodium hydroxide were added to adjust the solution to become more acidic or alkaline respectively. While the pH was modified in increments of 1 pH unit between pH 1.0 and pH 12.0, to investigate more closely 0.5 pH unit increments were adopted in between pH 4 and 6 with metal concentration of 400 μg/L of each metal. As the solutions became more acidic or alkaline, disappearance of peaks and changes in peak amplitude and potential were observed (Fig. 6b). At pH values below 3.0 or above 11.0, the Cd^{2+} stripping peak disappeared, but was visible otherwise. Conversely, Pb^{2+} and Hg^{2+} peaks were measurable at acidic pH values but were no longer measurable at pH 6.0 and above. At pH 12.0, none of the metal peaks were detectable. The weak stripping signal at lower pH may be due to the reduced ionization degree and thus fewer ion-exchange sites, while the decrease of the stripping signal at higher pH may be attributed to the hydrolysis of metal ions [50–52]. Interestingly, at pH 1.0 and pH 2.0, significantly greater peak currents were detected for Pb^{2+} and Hg^{2+}, while Cd^{2+} showed no response at all. This data supports the idea that pH stability is crucial for calibration and sensitivity of the sensor. This study also suggests that the ideal pH value for the co-detection of Cd^{2+}, Pb^{2+}, Hg^{2+} is between a pH value of 4.0 and 5.0, where all the three metal peaks are detectable and resolved. It is also noted that with increasing pH value the potential of the oxidation peak shifts more negatively for Cd^{2+} and Pb^{2+} or more positively for Hg^{2+}, mainly due to the reduction of hydrogen ions in the solution [15].

4.4. Metal sensing in soil and plant solutions

As a proof of concept, heavy metal measurements were conducted in plant and soil solutions using hand cleaved 0.94 mm Ø CFEs. The soil solution (TC = 22.76 mg/L) was diluted 1:1 vol% into 0.01 M acetate buffer (pH = 4.97) containing 50 mM NaCl to maintain the proper pH range of 4.0–5.0 and stirred at 2000 RPM for 5 minutes to ensure a homogenous mixture. Then heavy metals were added from 10 to 1600 μg/L. Fig. 7(a) shows measured current peaks using the DP-ASV method, where three distinct peaks for Cd^{2+}, Pb^{2+}, and Hg^{2+} were found at −0.75 V, −0.5 V, and +0.12 V respectively. Interestingly, even with organic carbon, clay, silt, and sand contents in the soil solution, the metal peak potentials were not shifted, showing good reproducibility between the buffer and soil solutions. However, the peak currents in the soil solution were much smaller in magnitude. As an example, Cd^{2+} has an amplitude of ~11 μA in the soil solution at 1600 μg/L concentration (Fig. 7(a)), whereas it was about 4 times higher to around 42 μA in the acetate buffer solution (Fig. 3(a)). In the acetate buffer solution, Hg^{2+} peaks were always dominant over the other two metal peaks. However, for the soil solution, Pb^{2+} peaks are dominant. Good linearity was observed for all three metals in the concentration range of 10–1600 μg/L with R^2 of 0.991, 0.996, and 0.957 for Cd^{2+}, Pb^{2+}, and Hg^{2+}, respectively (n=1) (Fig. 7(b)).

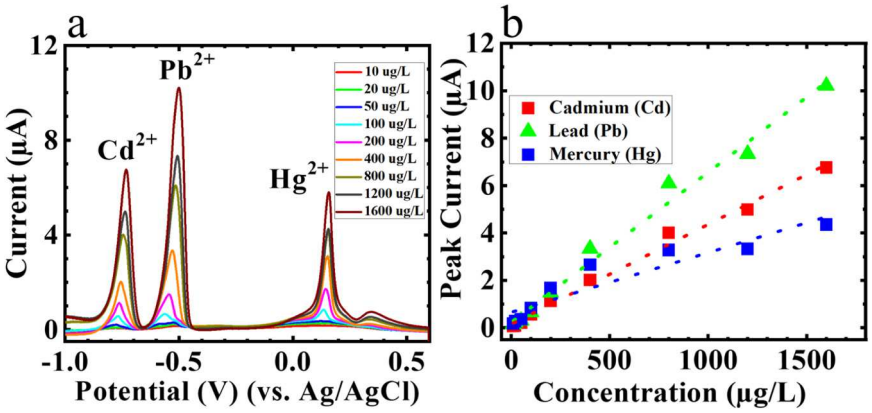

Fig. 8. (a) Detection of 10, 20, 50, 100, 200, 400, 800, 1200, and 1600 μg/L concentrations of Cd^{2+}, Pb^{2+}, and Hg^{2+} mixture in plant solution (pH=4.9) with CFE as WE. (b) Linear calibration curves in the mixture solution of Cd^{2+}, Pb^{2+}, and Hg^{2+} from 10 to 1600 μg/L (n=1).

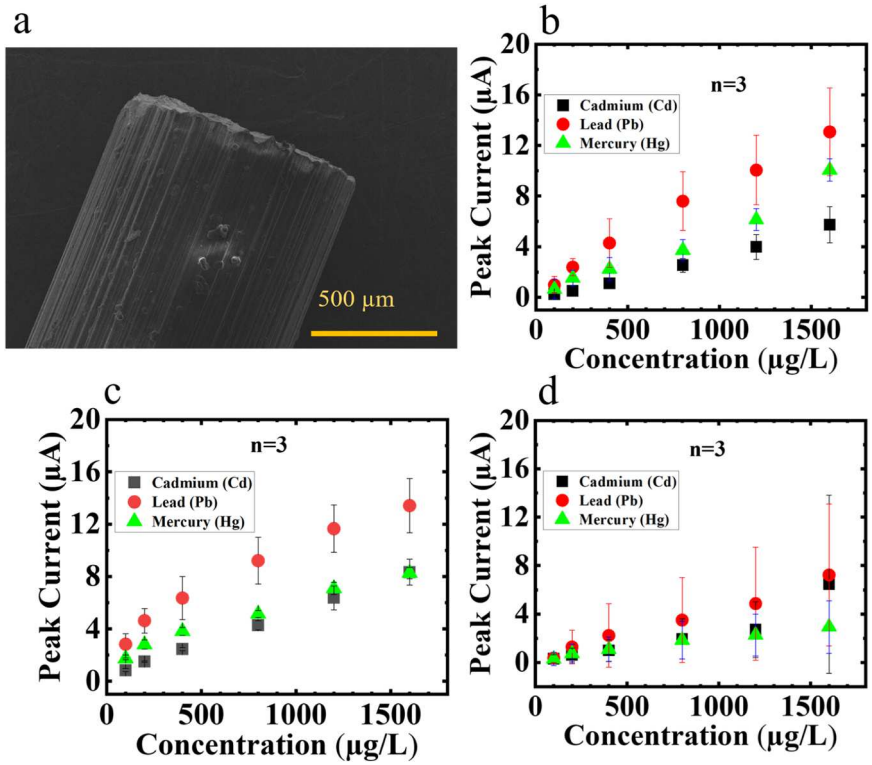

Fig. 9. Femtosecond laser cut CFE (a) SEM images of 0.94 mm CFE. Standard deviation among devices (n=3) for the detection of 100, 200, 400, 800, 1200, and 1600 μg/L concentration of Cd^{2+}, Pb^{2+}, and Hg^{2+} mixture in (b) 0.01 M acetate buffer (pH=4.97) solution containing 50 mM NaCl (c) soil solution (pH=5.03), and (d) in plant solution (pH=4.9) with CFE as WE. Error bar: standard deviation for n=3.

Similar to the soil solution, the plant solution (TC = 674.92 mg/L) was also diluted 1:1 vol% into 0.01 M acetate buffer (pH=4.97) containing 50 mM NaCl and stirred at 2000 RPM for 5 minutes to ensure a homogenous mixture. The metals were added from 10 to 1600 μg/L. Fig. 8(a) shows measured current peaks using the DP-ASV method, where three distinct peaks for Cd^{2+}, Pb^{2+}, and Hg^{2+} were found at −0.75 V, −0.5 V, and +0.12 V, respectively. Here as well, the corresponding peak potentials did not change when the solution type was changed. Again, compared to the buffer and soil solutions, the current peaks in the plant solution were significantly smaller. The 1600 μg/L concentration Cd^{2+} peak in the plant solution is ~7 μA in amplitude (Fig. 8(a)), whereas for the soil solution it was it was ~11 μA and for the buffer solution it was 42 μA (Fig. 3(a)). This reduction in the peak current is due to matrix effects in the plant solution as the solution likely contains carbon components such as proteins, fats, and lipids. This is also attributed to the measured TC values in the prepared solutions where the plant solution has 30 times higher carbon components than the soil solution. As with the soil solution, the Pb^{2+} peaks dominate the other two. Fig. 8(b) shows good linearity in the range of 10–400 μg/L for all three metals, beyond which the Hg^{2+} response became saturated with R^2 of 0.992, 0.988, and 0.873 for Cd^{2+}, Pb^{2+}, and Hg^{2+}, respectively (n=1).

4.5. *Repeatability of the CFEs*

The hand cleaving process is manual and delamination of the parylene-C on the CFE surface occurred frequently. Moreover, batch fabrication is cumbersome using this manual process, therefore a laser

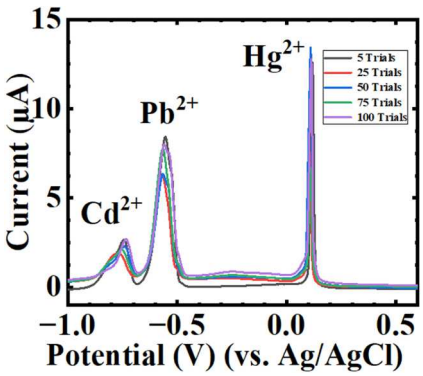

Fig. 10. Detection of 400 μg/L concentration of Cd^{2+}, Pb^{2+}, and Hg^{2+} mixture in 0.01 M acetate buffer (pH=4.97) solution over 100 trials.

cut method was introduced to check the reproducibility of the CFEs for heavy metal detection. Fig. 9(a) shows an SEM image of the sensing tip of an FS laser cut 0.94 mm Ø CFE, where a smooth cutting edge is observed compared to the earlier hand cleaved method sensing tip SEM (Fig. 1c). Using this FS laser cut 0.94 mm CFE, measurements were made from 100 to 1600 μg/L of Cd^{2+}, Pb^{2+}, and Hg^{2+} solutions using the DP-ASV buffer, soil, and plant solutions. The solutions were prepared following the same procedure described in Section 4.1 for buffer and Section 4.4 for soil and plant solutions. Similar to the hand cleaved CFEs, distinguishable stripping currents were measured for the FS cut CFEs at −0.75 V, −0.5 V, and +0.12 V for Cd^{2+}, Pb^{2+}, and Hg^{2+} respectively and maintained a linear response with increasing concentration measurements. Linearity among the metal peaks and the standard deviations of three CFEs are shown in the Fig. 9(b) for the buffer solutions with R^2 of 0.983, 0.981, and 0.965 for Cd^{2+}, Pb^{2+}, and Hg^{2+}, respectively, Fig. 9 (c) for the soil simulated solutions with R^2 of 0.992, 0.968, and 0.981 for Cd^{2+}, Pb^{2+}, and Hg^{2+}, respectively, and Fig. 9(d) for the plant simulated solutions with R^2 of 0.951, 0.962, and 0.959 for Cd^{2+}, Pb^{2+}, and Hg^{2+}, respectively. To check the capability of prolonged measurements, the FS cut 0.94 mm Ø CFE was used as WE in 400 μg/L concentrations of Cd^{2+}, Pb^{2+}, and Hg^{2+} solutions for 100 repeated DP-ASV measurements in the same buffer solution. Fig. 10 shows three distinct peaks for Cd^{2+}, Pb^{2+}, and Hg^{2+}. Although there is a little variation in the metal peaks amplitude, the change is not significant from the initial run to the 100th run. Moreover, no delamination of the carbon fibers was observed in the CFEs surface after 100 repetitive runs. This test confirms the reproducibility and electrode stability in the heavy metal measurements. Moreover, electrochemical cleaning is possible in the carbon fibers to renew their surfaces. This process can be done by applying an etching potential in order to gently etch the outer surface and renew the carbon fiber electrode by oxidizing and stripping plated metal off the surface [39,40]. This process will be applied in our future study to further enhance the CFE's stability.

In contrast to alternative heavy metal sensing electrodes like mercury-based electrodes and other carbon materials-based electrodes, our custom-fabricated CFE offers a cost-effective, environmentally friendly, and straightforward manufacturing process that consistently delivers metal sensing performance. Furthermore, our CFE meets the limit of detection standards outlined by the WHO. Fig. 11 illustrates a comparative analysis between our CFE and other widely used electrodes in a spider schematic diagram.

5. Conclusion

Here, we have developed a non-toxic, eco-friendly, and cost-effective sensing method to detect microgram per liter levels of cadmium (Cd^{2+}), lead (Pb^{2+}) and inorganic mercury (Hg^{2+}) metals in buffer, plant, and soil solutions using microfabrication-free CFEs. This sensor shows good sensitivity in a variety of solutions, with a wide range of metal concentrations from 10 to 1600 μg/L. We also extensively investigated the

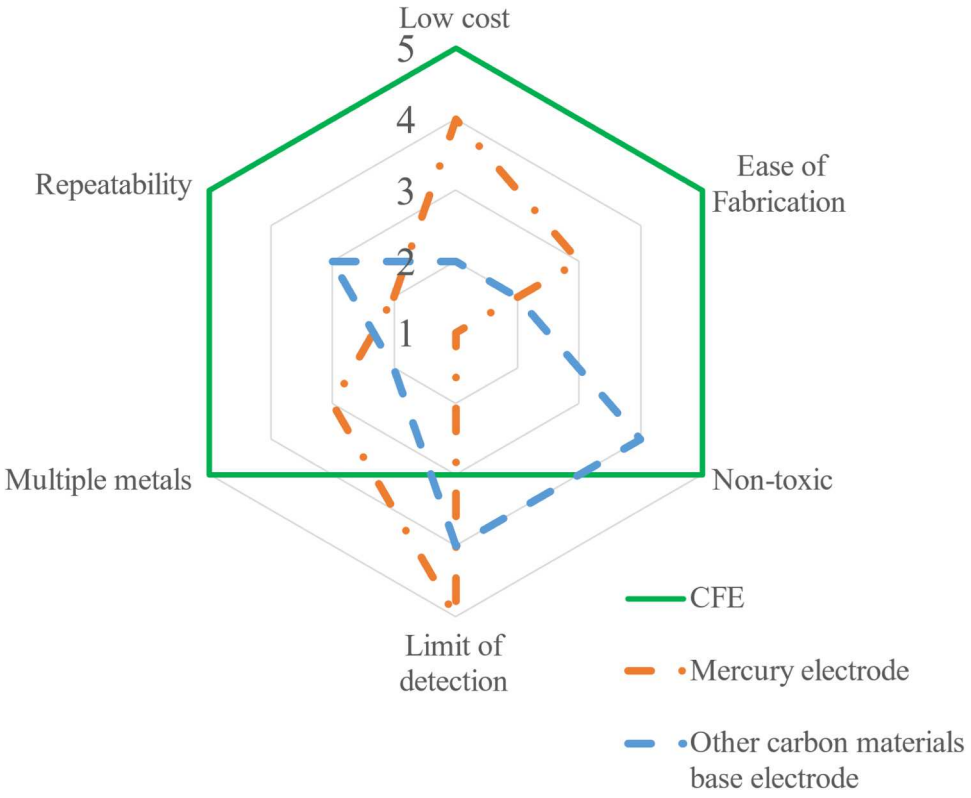

Fig. 11. Spider schematic compares toxicity, ease of fabrication, cost, repeatability, multiple metals detection ability and limit of detection performances among reported carbon fiber electrode (CFE), Hanging mercury electrode, and other carbon materials-based electrodes.

effect of solution pH and found a preferred pH range from pH 4.0–5.0 where all metal ions are stable and can be detected in a single run. For prolonged measurements, one CFE was used for 100 trials and showed good repeatability. This CFE sensor will allow non-toxic and cost-effective in-situ prolonged measurement of heavy metals in the environment. Future works involve integrating real-time data processing and wireless transmission to ensure remote monitoring applications.

CRediT authorship contribution statement

G M Hasan Ul Banna: Writing – review & editing, Writing – original draft, Visualization, Validation, Software, Resources, Project administration, Methodology, Investigation, Formal analysis, Data curation, Conceptualization. **James Siegenthaler:** Writing – review & editing, Methodology, Investigation, Funding acquisition, Conceptualization. **Antryg Benedict:** Writing – review & editing, Investigation. **Brendan Allen:** Writing – review & editing, Software, Data curation. **Raul Murillo Martinez:** Writing – review & editing, Investigation, Data curation. **Wei Zhang:** Writing – review & editing, Supervision, Methodology, Investigation, Formal analysis, Conceptualization. **Wen Li:** Writing – review & editing, Writing – original draft, Visualization, Validation, Supervision, Software, Resources, Project administration, Methodology, Investigation, Funding acquisition, Formal analysis, Data curation, Conceptualization.

Declaration of Competing Interest

The authors declare that they have no known competing financial interests or personal relationships that could have appeared to influence the work reported in this paper.

Data Availability

Data will be made available on request.

Acknowledgements

This work was supported by the National Science Foundation (Award Number: 2226500).

Appendix A. Supporting information

Supplementary data associated with this article can be found in the online version at doi:10.1016/j.sna.2024.115232.

References

[1] G.E. Brown Jr, A.L. Foster, J.D. Ostergren, Mineral surfaces and bioavailability of heavy metals: a molecular-scale perspective, Proc. Natl. Acad. Sci. 96 (1999) 3388–3395.
[2] Ogwuegbu Duruibe, Heavy Egwurugwu, metal pollution and human biotoxic effects, Int. J. Phys. Sci. 2 (2007) 112–118.
[3] N.K. Srivastava, C.B. Majumder, Novel biofiltration methods for the treatment of heavy metals from industrial wastewater, J. Hazard. Mater. 151 (2008) 1–8, https://doi.org/10.1016/j.jhazmat.2007.09.101.
[4] R. Goyer, Issue paper on the human health effects of metals: US Environmental Protection Agency, 2004 - Google Search, (n.d.). https://www.google.com/search?q=R.+Goyer%2C+Issue+paper+on+the+human+health+effects+of+metals%3A+US+Environmental+Protection+Agency%2C+2004&rlz=1C1RXQR_enUS979US979&oq=R.+Goyer%2C+Issue+paper+on+the+human+health+effects+of+metals%3A+US+Environmental+Protection+Agency%2C+2004&aqs=chrome.69i57.248j0j9&sourceid=chrome&ie=UTF-8 (accessed June 2, 2023).
[5] A. Zwolak, M. Sarzyńska, E. Szpyrka, K. Stawarczyk, Sources of soil pollution by heavy metals and their accumulation in vegetables: a review, Water Air Soil Pollut. 230 (2019) 1–9.
[6] M. Uchimiya, D. Bannon, H. Nakanishi, M.B. McBride, M.A. Williams, T. Yoshihara, Chemical speciation, plant uptake, and toxicity of heavy metals in agricultural soils, J. Agric. Food Chem. 68 (2020) 12856–12869.
[7] P. Punia, M.K. Bharti, R. Dhar, P. Thakur, A. Thakur, Recent advances in detection and removal of heavy metals from contaminated water, ChemBioEng Rev. 9 (2022) 351–369, https://doi.org/10.1002/cben.202100053.
[8] T.O. Hara, B. Singh, Electrochemical biosensors for detection of pesticides and heavy metal toxicants in water: recent trends and progress, ACS EST Water 1 (2021) 462–478, https://doi.org/10.1021/acsestwater.0c00125.
[9] O.B. Akpor, G.O. Ohiobor, D.T. Olaolu, Heavy metal pollutants in wastewater effluents: sources, effects and remediation, Adv. Biosci. Bioeng. 2 (2014) 37–43.
[10] E.M. Alissa, G.A. Ferns, Heavy metal poisoning and cardiovascular disease, J. Toxicol. 2011 (2011) e870125, https://doi.org/10.1155/2011/870125.
[11] H.S. Kim, Y.J. Kim, Y.R. Seo, An overview of carcinogenic heavy metal: molecular toxicity mechanism and prevention, J. Cancer Prev. 20 (2015) 232–240, https://doi.org/10.15430/JCP.2015.20.4.232.
[12] G.H. Parker, C.E. Gillie, J.V. Miller, D.E. Badger, M.L. Kreider, Human health risk assessment of arsenic, cadmium, lead, and mercury ingestion from baby foods, Toxicol. Rep. 9 (2022) 238–249, https://doi.org/10.1016/j.toxrep.2022.02.001.
[13] HoR: Baby foods are tainted with dangerous levels. - Google Scholar, (n.d.). https://scholar.google.com/scholar_lookup?title=Baby%20Foods%20are%20Tainted%20With%20Dangerous%20Levels%20of%20Arsenic%2C%20Lead%2C%20Cadmium%20and%20Mercury%3A%20Staff%20Report&publication_year=2021&author=ECP (accessed June 2, 2023).
[14] W. Gao, H.Y.Y. Nyein, Z. Shahpar, H.M. Fahad, K. Chen, S. Emaminejad, Y. Gao, L.-C. Tai, H. Ota, E. Wu, J. Bullock, Y. Zeng, D.-H. Lien, A. Javey, Wearable microsensor array for multiplexed heavy metal monitoring of body fluids, ACS Sens 1 (2016) 866–874, https://doi.org/10.1021/acssensors.6b00287.
[15] A.J. Borrill, N.E. Reily, J.V. Macpherson, Addressing the practicalities of anodic stripping voltammetry for heavy metal detection: a tutorial review, Analyst 144 (2019) 6834–6849, https://doi.org/10.1039/C9AN01437C.
[16] X. Mo, M.G. Siebecker, W. Gou, L. Li, W. Li, A review of cadmium sorption mechanisms on soil mineral surfaces revealed from synchrotron-based X-ray absorption fine structure spectroscopy: Implications for soil remediation, Pedosphere 31 (2021) 11–27, https://doi.org/10.1016/S1002-0160(20)60017-0.
[17] K.S. Rao, T. Balaji, T.P. Rao, Y. Babu, G.R.K. Naidu, Determination of iron, cobalt, nickel, manganese, zinc, copper, cadmium and lead in human hair by inductively coupled plasma-atomic emission spectrometry, Spectrochim. Acta Part B: At. Spectrosc. 57 (2002) 1333–1338.
[18] S. Munro, L. Ebdon, D.J. McWeeny, Application of inductively coupled plasma mass spectrometry (ICP-MS) for trace metal determination in foods, J. Anal. . Spectrom. 1 (1986) 211–219, https://doi.org/10.1039/JA9860100211.
[19] R.K. Soodan, Y.B. Pakade, A. Nagpal, J.K. Katnoria, Analytical techniques for estimation of heavy metals in soil ecosystem: a tabulated review, Talanta 125 (2014) 405–410, https://doi.org/10.1016/j.talanta.2014.02.033.
[20] C.M.A. Brett, Electrochemical sensors for environmental monitoring. Strategy and examples, Pure Appl. Chem. 73 (2001) 1969–1977, https://doi.org/10.1351/pac200173121969.
[21] Y. Lu, X. Liang, C. Niyungeko, J. Zhou, J. Xu, G. Tian, A review of the identification and detection of heavy metal ions in the environment by voltammetry, Talanta 178 (2018) 324–338.
[22] T.R. Copeland, R.K. Skogerboe, Anodic stripping voltammetry, Anal. Chem. 46 (1974) 1257A–1268a.
[23] E.A. McGaw, G.M. Swain, A comparison of boron-doped diamond thin-film and Hg-coated glassy carbon electrodes for anodic stripping voltammetric determination of heavy metal ions in aqueous media, Anal. Chim. Acta 575 (2006) 180–189, https://doi.org/10.1016/j.aca.2006.05.094.
[24] J. Wang, Stripping analysis at bismuth electrodes: a review, Electroanal.: Int. J. Devoted Fundam. Pract. Asp. Electroanal. 17 (2005) 1341–1346.
[25] A. Giacomino, A. Ruo Redda, S. Squadrone, M. Rizzi, M.C. Abete, C. La Gioia, R. Toniolo, O. Abollino, M. Malandrino, Anodic stripping voltammetry with gold electrodes as an alternative method for the routine determination of mercury in fish. Comparison with spectroscopic approaches, Food Chem. 221 (2017) 737–745, https://doi.org/10.1016/j.foodchem.2016.11.111.
[26] K.Z. Brainina, Film stripping voltammetry, Talanta 18 (1971) 513–539.
[27] S.E. Ward Jones, F.G. Chevallier, C.A. Paddon, R.G. Compton, General theory of cathodic and anodic stripping voltammetry at solid electrodes: mathematical modeling and numerical simulations, Anal. Chem. 79 (2007) 4110–4119.
[28] D. Menshykau, R.G. Compton, Influence of electrode roughness on stripping voltammetry: mathematical modeling and numerical simulation, J. Phys. Chem. C 113 (2009) 15602–15620.
[29] O.S. Ivanova, F.P. Zamborini, Electrochemical size discrimination of gold nanoparticles attached to glass/indium- tin-oxide electrodes by oxidation in bromide-containing electrolyte, Anal. Chem. 82 (2010) 5844–5850.
[30] D.K. Pattadar, J.N. Sharma, B.P. Mainali, F.P. Zamborini, Impact of the assembly method on the surface area-to-volume ratio and electrochemical oxidation potential of metal nanospheres, J. Phys. Chem. C. 123 (2019) 24304–24312, https://doi.org/10.1021/acs.jpcc.9b06555.
[31] M.L. Huffman, B.Jill Venton, Carbon -fiber microelectrodes for in vivo applications, Analyst 134 (2009) 18–24, https://doi.org/10.1039/B807563H.
[32] F. Scholz, Electroanalytical Methods, Springer, 2010.
[33] Glassy carbon as electrode material in electro- analytical chemistry, Glassy Carbon as Electrode Material in Electro- Analytical Chemistry (n.d.). https://doi.org/10.1016/S0003-2670(00)00025-8.
[34] Md.A. Rahman, M.-S. Won, Y.-B. Shim, Characterization of an EDTA bonded conducting polymer modified electrode: its application for the simultaneous determination of heavy metal ions, Anal. Chem. 75 (2003) 1123–1129, https://doi.org/10.1021/ac0262917.
[35] X. Liu, Y. Yao, Y. Ying, J. Ping, Recent advances in nanomaterial-enabled screen-printed electrochemical sensors for heavy metal detection, TrAC Trends Anal. Chem. 115 (2019) 187–202, https://doi.org/10.1016/j.trac.2019.03.021.

[36] A.K. Wanekaya, Applications of nanoscale carbon-based materials in heavy metal sensing and detection, Analyst 136 (2011) 4383–4391, https://doi.org/10.1039/C1AN15574A.
[37] J. Lee, S. Kim, H. Shin, Hierarchical porous carbon electrodes with sponge-like edge structures for the sensitive electrochemical detection of heavy metals, Sensors 21 (2021) 1346, https://doi.org/10.3390/s21041346.
[38] W. Ye, Y. Li, J. Wang, B. Li, Y. Cui, Y. Yang, G. Qian, Electrochemical detection of trace heavy metal ions using a Ln-MOF modified glass carbon electrode, J. Solid State Chem. 281 (2020) 121032, https://doi.org/10.1016/j.jssc.2019.121032.
[39] P. Takmakov, M.K. Zachek, R.B. Keithley, P.L. Walsh, C. Donley, G.S. McCarty, R. M. Wightman, Carbon microelectrodes with a renewable surface, Anal. Chem. 82 (2010) 2020–2028, https://doi.org/10.1021/ac902753x.
[40] M.L.A.V. Heien, P.E.M. Phillips, G.D. Stuber, A.T. Seipel, R.Mark Wightman, Overoxidation of carbon-fiber microelectrodes enhances dopamine adsorption and increases sensitivity, Analyst 128 (2003) 1413–1419, https://doi.org/10.1039/B307024G.
[41] H. Rafi, A.G. Zestos, Review—Recent advances in FSCV detection of neurochemicals via waveform and carbon microelectrode modification, J. Electrochem. Soc. 168 (2021) 057520, https://doi.org/10.1149/1945-7111/ac0064.
[42] J. Wang, J. Lu, S.B. Hocevar, P.A.M. Farias, B. Ogorevc, Bismuth-coated carbon electrodes for anodic stripping voltammetry, Anal. Chem. 72 (2000) 3218–3222, https://doi.org/10.1021/ac000108x.
[43] M. Slavec, S.B. Hocevar, L. Baldrianova, E. Tesarova, I. Svancara, B. Ogorevc, K. Vytras, Antimony film microelectrode for anodic stripping measurement of Cadmium(II), Lead(II) and Copper(II), Electroanalysis 22 (2010) 1617–1622, https://doi.org/10.1002/elan.200900583.
[44] Y. Li, J.B. Sallach, W. Zhang, S.A. Boyd, H. Li, Characterization of plant accumulation of pharmaceuticals from soils with their concentration in soil pore water, Environ. Sci. Technol. 56 (2022) 9346–9355, https://doi.org/10.1021/acs.est.2c00303.
[45] J.R. Siegenthaler, B.C. Gushiken, D.F. Hill, S.L. Cowen, M.L. Heien, Moving fast-scan cyclic voltammetry toward FDA compliance with capacitive decoupling patient protection, ACS Sens. 5 (2020) 1890–1899, https://doi.org/10.1021/acssensors.9b02249.
[46] A. Mourya, B. Mazumdar, S.K. Sinha, Determination and quantification of heavy metal ion by electrochemical method, J. Environ. Chem. Eng. 7 (2019) 103459, https://doi.org/10.1016/j.jece.2019.103459.
[47] International Committee on Harmonization, Validation of Analytical Procedures: Text and Methodology, Q2(R1), Nov. 2005. - Google Search, (n.d.). https://www.google.com/search?q=International+Committee+on+Harmonization%2C+%E2%80%9CValidation+of+Analytical+Procedures%3A+Text+and+Methodology%2C+Q2(R1)%2C+Nov.+2005.&rlz=1C1RXQR_enUS979US979&oq=International+Committee+on+Harmonization%2C+%E2%80%9CValidation+of+Analytical+Procedures%3A+Text+and+Methodology%2C+Q2(R1)%2C+Nov.+2005.&gs_lcrp=EgZjaHJvbWUyBggAEEUYOdIBBzIzOGowajGoAgCwAgA&sourceid=chrome&ie=UTF-8 (accessed February 6, 2024).
[48] R. Trouillon, Y. Lin, L.J. Mellander, J.D. Keighron, A.G. Ewing, Evaluating the diffusion coefficient of dopamine at the cell surface during amperometric detection: disk vs ring microelectrodes, Anal. Chem. 85 (2013) 6421–6428, https://doi.org/10.1021/ac400965d.
[49] L.T. Tran, H.V. Tran, H.H. Cao, T.H. Tran, C.D. Huynh, Electrochemically effective surface area of a polyaniline nanowire-based platinum microelectrode and development of an electrochemical DNA sensor, J. Nanotechnol. 2022 (2022) e8947080, https://doi.org/10.1155/2022/8947080.
[50] C. Gao, X.-Y. Yu, R.-X. Xu, J.-H. Liu, X.-J. Huang, AlOOH-reduced graphene oxide nanocomposites: one-pot hydrothermal synthesis and their enhanced electrochemical activity for heavy metal ions, ACS Appl. Mater. Interfaces 4 (2012) 4672–4682, https://doi.org/10.1021/am3010434.
[51] L. Shi, Y. Li, X. Rong, Y. Wang, S. Ding, Facile fabrication of a novel 3D graphene framework/Bi nanoparticle film for ultrasensitive electrochemical assays of heavy metal ions, Anal. Chim. Acta 968 (2017) 21–29, https://doi.org/10.1016/j.aca.2017.03.013.
[52] Y. Wei, R. Yang, X. Chen, L. Wang, J.-H. Liu, X.-J. Huang, A cation trap for anodic stripping voltammetry: NH3–plasma treated carbon nanotubes for adsorption and detection of metal ions, Anal. Chim. Acta 755 (2012) 54–61, https://doi.org/10.1016/j.aca.2012.10.021.

G M Hasan Ul Banna is a graduate student at the Microtechnology Lab in the Electrical and Computer Engineering Department of Michigan State University. He has been doing research with Professor Wen Li since Summer 2021. So far, he has published four conference proceedings and one journal paper. Earlier, Mr. Banna completed his MS in Electronic Engineering from South Korea and a Bachelor's in Electrical and Electronic Engineering from Bangladesh.

Dr. James Siegenthaler is a Scientist at Fraunhofer USA Center Midwest, East Lansing, MI, USA. He is a graduate of University of Arizona with a PhD in Analytical Chemistry focusing on instrument design and development for neurochemical measurements of dopamine in the brain. James has a diverse background from spectroscopic techniques to study chemical species in solution, to quantifying pesticides in commercial products, and understanding the surface phenomenon of materials through AFM and SEM characterization.

Antryg Benedict received his BSc degree in Chemistry with a minor in Geology from George Mason University in 2021. He is currently pursuing his PhD degree in Crop and Soil Sciences at Michigan State University. His research uses molecular dynamics to study the infectious prion protein's interactions with geosorbent materials and heavy metals.

Brendan Allen is a final year student at Michigan State University, where he is pursuing a bachelor's degree in chemical engineering. He is currently working as an intern at Fraunhofer USA Center Midwest, East Lansing, MI, USA.

Raul Ernesto Murillo is currently in his second year at Michigan State University, where he is pursuing a bachelor's degree in mechanical engineering with a specialization in Biomedical Engineering. He hails from Tegucigalpa, Honduras, where he spent his formative years and completed his high school education at the American School of Tegucigalpa.

Dr. Wei Zhang is an Associate Professor of Environmental Soil Physics in the Department of Plant, Soil and Microbial Sciences at Michigan State University, USA. He received his Ph. D. degree in Environmental Engineering from Cornell University in 2010, his MS degree in Biosystems Engineering from Oklahoma State University in 2006, and his bachelor's degree in Environmental Chemistry from Nanjing University in 2000. His research focuses on environmental processes and impacts of environmental contaminants (e.g., engineered nanoparticles, pharmaceuticals, antibiotic resistance genes, prions, per- and polyfluoroalkyl substances, and toxic metals) in agroecosystems.

Dr. Wen Li received the B.S. degree in material science and engineering from Tsinghua University, Beijing, and the M.S. and Ph.D. degrees both in electrical engineering from California Institute of Technology, Pasadena, in 2004 and 2009, respectively. She joined Michigan State University, East Lansing, in 2009 and is currently a Professor in the Department of Electrical and Computer Engineering. She also holds a courtesy appointment in the Department of Biomedical Engineering. Her research interests include MEMS/NEMS technologies and systems, micro sensors and actuators, biomimetic devices and systems, microfluidic and lab-on-chip systems, and microsystem integration and packaging technologies.